

Isolation and Reactivity of Arylnickel(II) Complexes in Nickel-Catalyzed Borylation of Aryl Fluorosulfates

Manoj Kumar Sahoo, Jeong Woo Lee, Soochan Lee, Wonyoung Choe, Byunghyuck Jung,* Jaesung Kwak,* and Sung You Hong*



Cite This: *JACS Au* 2024, 4, 1646–1653



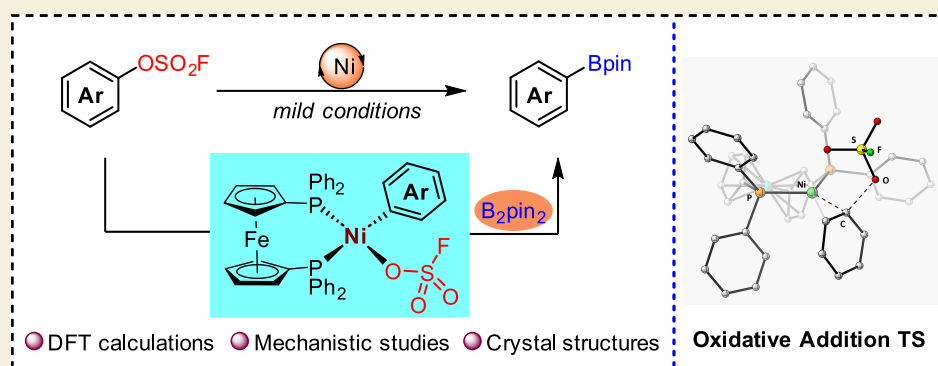
Read Online

ACCESS |

Metrics & More

Article Recommendations

Supporting Information



ABSTRACT: Aryl fluorosulfates have emerged as versatile SuFExable substrates, harnessing the reactivity of the S–F bond. In this study, we unveil their alternative synthetic utility in nickel-catalyzed borylation via C–O bond activation. This method highlights mild reaction conditions, a broad substrate scope, and moderate functional group tolerance, rendering it a practical and appealing approach for synthesizing a diverse array of aryl boronate esters. Furthermore, computational analysis sheds light on the reaction pathways, uncovering the participation of LNi(0) and LNi(II)ArX species. This insight is supported by the ^{31}P NMR reaction monitoring along with isolation and single-crystal X-ray structural elucidation of well-defined arylnickel(II) intermediates obtained from the oxidative addition of aryl fluorosulfates. A comprehensive investigation, merging experimental and computational approaches, deepens our understanding of the alternative reactivity of SuFExable substrates.

KEYWORDS: aryl fluorosulfates, computational studies, intermediate isolation, nickel catalysis, organoborons

1. INTRODUCTION

Organoborons have gained recognition as key organometallic reagents owing to their synthetic versatility, bench stability, low toxicity, and ease of handling.^{1–6} Recent progress in palladium-catalyzed C–B bond formation, including the Miyaura borylation of aryl halides, has paved the way for the establishment of straightforward and reliable routes to prepare arylboron compounds.^{7–10} However, comparatively less attention has been focused on elucidating the reaction pathways in nickel-catalyzed processes.^{11,12} Nickel catalysts, in addition to being cost-effective, exhibit superior performance compared to palladium ones in activating less reactive electrophiles such as pseudohalides, esters, or even ethers.^{13,14} Despite these advantages, nickel can exist in diverse oxidation states, and the facile interconversion between these states can pose challenges in controlling the desired reactivity.^{15–19} Furthermore, the requirement of relatively high catalyst loading limits the practical application of nickel catalysis. Therefore, gaining a comprehensive understanding of the reaction mechanism, especially when it involves the activation of C–O bonds, is crucial.

Due to the affordability and widespread availability, phenol derivatives have been employed as alternatives for aryl halides in the development of deoxygenative cross-coupling reactions.^{20–23} However, a limited number of borylation reactions utilizing phenol derivatives have been reported under photoredox or first-row transition-metal catalysis.^{8,24–29} This is due to the tendency of the resulting arylborons to further react with phenol derivatives, forming undesired dimerized products via cross-coupling reactions. The lack of detailed mechanistic understanding regarding key elementary reaction steps leaves room for further exploration in deoxygenative borylation using phenol derivatives.

Received: February 12, 2024

Revised: March 6, 2024

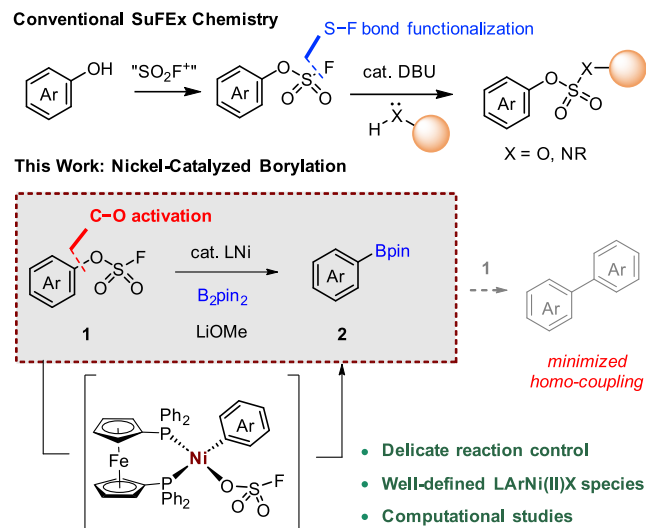
Accepted: March 11, 2024

Published: March 25, 2024



After the pioneering development of the sulfur(VI) fluoride exchange (SuFEx) chemistry by Sharpless and co-workers,^{30–33} aryl fluorosulfates have found extensive use in ligation or polymerization reactions (Scheme 1). Aryl fluorosulfates show

Scheme 1. Catalytic S–F vs C–O Bond Activation of Aryl Fluorosulfates



excellent stability against hydrolysis and thermolysis when compared to sulfonyl halides.³⁰ These advantages of aryl fluorosulfates have enabled their exploration as a convenient source of electrophiles within catalytic reactions.^{34–39} However, there is a lack of experimental characterization of well-defined nickel complexes within catalytic cycles. Herein, we present an efficient deoxygenative borylation of aryl fluorosulfates under mild conditions, achieved through nickel-catalyzed C–O bond activation instead of the typical S–F bond cleavage in SuFEx chemistry. To gain insights into the reaction mechanism, we employed a combined experimental and computational approach to elucidate the elementary reaction steps in this nickel catalysis.

2. RESULTS AND DISCUSSION

2.1. Reaction Optimization

We began our investigation of the Ni-catalyzed borylation reaction using 4-methoxyphenyl fluorosulfate (**1a**) as a model substrate (Table 1). After rigorous optimization of the reaction parameters (see also Supporting Information, Section III-2), to our delight, the borylation proceeded efficiently under mild reaction conditions at a temperature of 40 °C. By employing 5 mol % each of Ni(COD)₂ and 1,1'-bis(diphenylphosphino)ferrocene (dppf), the desired boronic ester **2a** was obtained in 82% GC yield after 24 h (Table 1, entry 1). Notably, the C–O activation of the methoxy substituent was not observed. In addition, no side products associated with the S–F activation of the fluorosulfate moiety were observed. Moreover, the reaction required near equimolar amounts of B₂pin₂ (1.1 equiv) and LiOMe (1.25 equiv) with the optimal solvent, 1,2-dimethoxyethane (1,2-DME). The presence of both a base and a ligand was found to be crucial for the reaction, as evidenced by the formation of only traces of the desired product **2a** in their absence (entry 2). No desired product was observed without the nickel source (entry 3). Moreover, dppf was found to be the most efficient ligand for yielding **2a**, while all other *P,P* or *N,N*-

Table 1. Reaction Optimization^{a,b}

entry	variation from initial conditions	yield (%) ^a
1	none	82
2	no base or no ligand	trace
3	no Ni(COD) ₂	0
4	dcpe instead of dppf	27
5	xantphos instead of dppf	29
6	NiCl ₂ glyme instead of Ni(COD) ₂	50
7	(Me ₃ P) ₂ NiCl ₂ as catalyst	46
8	(dcpe)Ni(COD) (Ni1) as catalyst	42
9	(dppf)NiCl ₂ as catalyst	48
10	(dppf)Ni(COD) (Ni2) as catalyst	88(71) ^b
11	Ni2 as catalyst at rt	61
12	2.5 mol % of Ni2 used	49

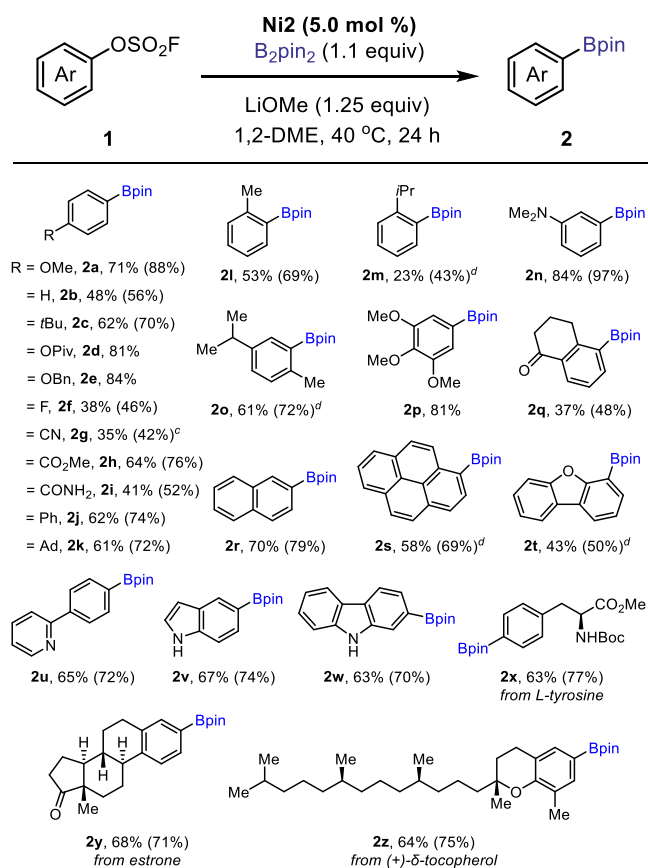
^aReaction conditions: **1a** (0.4 mmol), B₂pin₂ (0.44 mmol, 1.1 equiv), [Ni] (5.0 mol %), ligand (5.0 mol %), base (0.5 mmol, 1.25 equiv), and 1,2-DME (1.0 mL), 40 °C, 24 h. Yields were determined by analyzing the crude reaction mixture in GC-FID using *n*-dodecane as an internal standard. ^bIsolated yield in parentheses.

ligands were less efficient (entries 4 and 5, for more details, see also Supporting Information). Various nickel catalysts, including NiCl₂ glyme, (Me₃P)₂NiCl₂, (dcpe)Ni(COD) (**Ni1**), and (dppf)NiCl₂, afforded the product in moderate yields (entries 6–9). Similarly, among various solvents tested for this reaction, ethereal solvents were found to be effective and gave the desired product in high yields, while others showed poor yields (Table S1). The reaction efficiency was significantly affected by the choice of base, and except for LiOMe, other bases were found to be less effective in giving high product yields (Table S3). Notably, precomplexed catalyst (dppf)Ni(COD) (**Ni2**) afforded **2a** in higher yield (entry 10). However, when the reaction temperature was lowered to rt or the loading of **Ni2** was reduced to 2.5 mol %, the yield of **2a** was diminished to 61 and 49%, respectively (entries 11 and 12).

2.2. Reaction Scope

With the optimized conditions in hand, we next explored the scope of the borylation reactions (Table 2). Diverse (hetero)aryl fluorosulfates and fluorosulfurylated bioactive molecules smoothly underwent the borylation reactions, affording the corresponding products **2** in moderate-to-high yields. Phenyl boronate ester **2b** was isolated in a moderate yield of 48%. *Para*-substituted electron-rich aryl fluorosulfates bearing OMe, OBn, *t*Bu, or adamantyl groups gave the respective borylated products in 61–84% isolated yields (**2a**, **2c**, **2e**, and **2k**). Substrates with electron-withdrawing groups in the *para* position, such as *p*-OPiv, *p*-CO₂Me, and *p*-CONH₂, afforded the corresponding boronate esters **2d**, **2h**, and **2i** in moderate-to-good yields (41–81%). Additionally, *para*-phenyl-substituted **1j** gave **2j** in a 62% isolated yield. Notably, functional groups such as *p*-F and *p*-CN were also tolerated, providing their corresponding products **2f** and **2g**, albeit in low isolated yields. Substrates bearing *o*-Me and *o*-*i*Pr groups gave the boronate esters **2l** and **2m** in 53 and 23% isolated yields, respectively, possibly due to steric hindrance.

Furthermore, disubstituted **2o** and trisubstituted **2p** were isolated in yields of 61 and 81%, respectively. Interestingly, *meta*-substituted **2n** was obtained in a high isolated yield of 84%.

Table 2. Substrate Scope Study^{a,b}

^aReaction conditions: **1** (0.4 mmol), B₂pin₂ (0.44 mmol, 1.1 equiv), Ni₂ (5.0 mol %), LiOMe (0.5 mmol, 1.25 equiv), and 1,2-DME (1.0 mL), 40 °C, 24 h. ^bIsolated yields are provided, with the NMR yields given in parentheses using mesitylene as an internal standard. ^cDimerized product of **1g** was isolated in an 8% yield. ^dThe reaction was extended to 36 h using 2.0 equiv of B₂pin₂ and 2.5 equiv of LiOMe.

Remarkably, **1q** bearing ketone functionality was tolerated, giving the corresponding product **2q**, albeit in a low yield. Moreover, 2-naphthol-derived **1r** and pyrene derivative **1s** produced **2r** and **2s** in moderate yields. Additionally, this method demonstrated competence in the synthesis of heteroaromatic boronic esters, providing **2t–2w** in moderate-to-good yields. We further highlighted the synthetic utility of this nickel catalysis by conducting late-stage borylation of fluorosulfonylated derivatives of L-tyrosine (**1x**), estrone (**1y**), and (+)-δ-tocopherol (**1z**). This led to the successful formation of the corresponding borylated products **2x–2z** in good yields (63 to 68%).

2.3. Computational Investigations

To shed light on the detailed mechanism of this catalytic reaction, we performed density functional theory (DFT) calculations for the formation of **2b** as a model reaction, as depicted in Figure 1. The catalytic cycle is initiated by the endergonic displacement of the COD ligand of Ni₂ (denoted as NiI) to **1b**, generating η²-coordinated **Int-1**. Our calculation revealed that the oxidative addition proceeded through S_NAr-type TS (**TS-1**, Figure 2a), followed by rebound of OSO₂F anion (**Int-2**). The overall free-energy barrier for the oxidative addition is computed as 8.0 kcal/mol, and the formation of

Int-2 is exergonic by 20.3 kcal/mol. The experimental studies for the isolation of arylnickel(II) intermediate by the oxidative addition will be discussed *vide infra* (Section 2.4). While the anion exchange between the OSO₂F anion of **Int-2** and methoxide is favored by 6 kcal/mol, in our experimental observation, the corresponding **Int-2'** species could not be detected, whereas **Int-2** was readily observed. This discrepancy may be attributed to the preferential reactivity of lithium methoxide toward B₂pin₂, leading to the formation of boronate ester (B₂pin₂-LiOMe, **A**) and concurrent reduction of the effective concentration of free methoxide ions.

During our attempts to locate the transmetalation TS directly from **Int-2**, we found that the monodentate dppf ligation is required to structurally organize **A** into the proper orientation for the TS. The formation of **Int-3** from **Int-2** is slightly exergonic by 0.2 kcal/mol and the intermediate features square planar coordination, where the methoxide of **A** and the phenyl group are coordinated *trans* to phosphine and OSO₂F, respectively. Interestingly, OSO₂F and pinacol are bridged by the lithium cation, and Bpin is positioned at the axial position. In the transmetalation TS (**TS-2**, Figure 2b), the Bpin is transferred to the nickel center with simultaneous cleavage of the B–B bond of **A**, generating nickel boryl intermediate **Int-4**. Our calculation revealed that the transmetalation step is highly exergonic by 25.7 kcal/mol with the free-energy barrier of 15.1 kcal/mol, indicating that the transmetalation is the rate-limiting step. For the reductive elimination step, we removed LiOSO₂F and (MeO)Bpin from **Int-4** because these species are weakly bound to the nickel center. During the optimization process, we observed the bond formation between the phenyl group and the Bpin group. The resulting product-coordinated species (**Int-5**) features an η²-coordination mode, and monodentate dppf ligation and is 7.5 kcal/mol more stable than **Int-4**. The subsequent bidentate chelation of the dppf ligand is computed to be exergonic by 16.6 kcal/mol (**Int-6**), and the product displacement of **Int-6** with **1b** regenerates **Int-1**. From the reductive elimination of **Int-4** to the catalyst regeneration step, a thermodynamically downhill process of 29.1 kcal/mol was calculated. The high exergonicity of the energy profile may provide the driving force for this nickel catalysis under mild reaction conditions.

2.4. Experimental Investigations

To gain deeper insights into the reaction mechanism, we undertook efforts to prepare catalytic reaction intermediates that correspond to the proposed elementary reaction steps. Our initial attempt to capture the oxidative addition complex Ni³ from **1g** and NiI was unsuccessful due to its instability. We reasoned that the ligand exchange, replacing fluorosulfate with pivalate, may yield a more stabilized structure.⁴⁰ Notably, complex Ni³ was successfully isolated in a high yield using this indirect ligand exchange method (Figure 3a). The structure of Ni³ was unequivocally confirmed by single-crystal X-ray diffraction (XRD). Its characterization was also confirmed by comparing the spectroscopic data of the complex directly prepared from **3** with NiI via oxidative addition, according to the Itami group's procedure.^{40,41}

Furthermore, the reaction progress between **1g** and NiI in the presence of CsOPiv was monitored by ³¹P NMR analysis (Figure 3b). Within 10 min of the reaction, two sets of clear doublets evolved as indicated in the ³¹P NMR spectra along with the characteristic singlet from unreacted NiI. One set of doublets at chemical shifts of 70.9 and 57.5 ppm, assigned to the

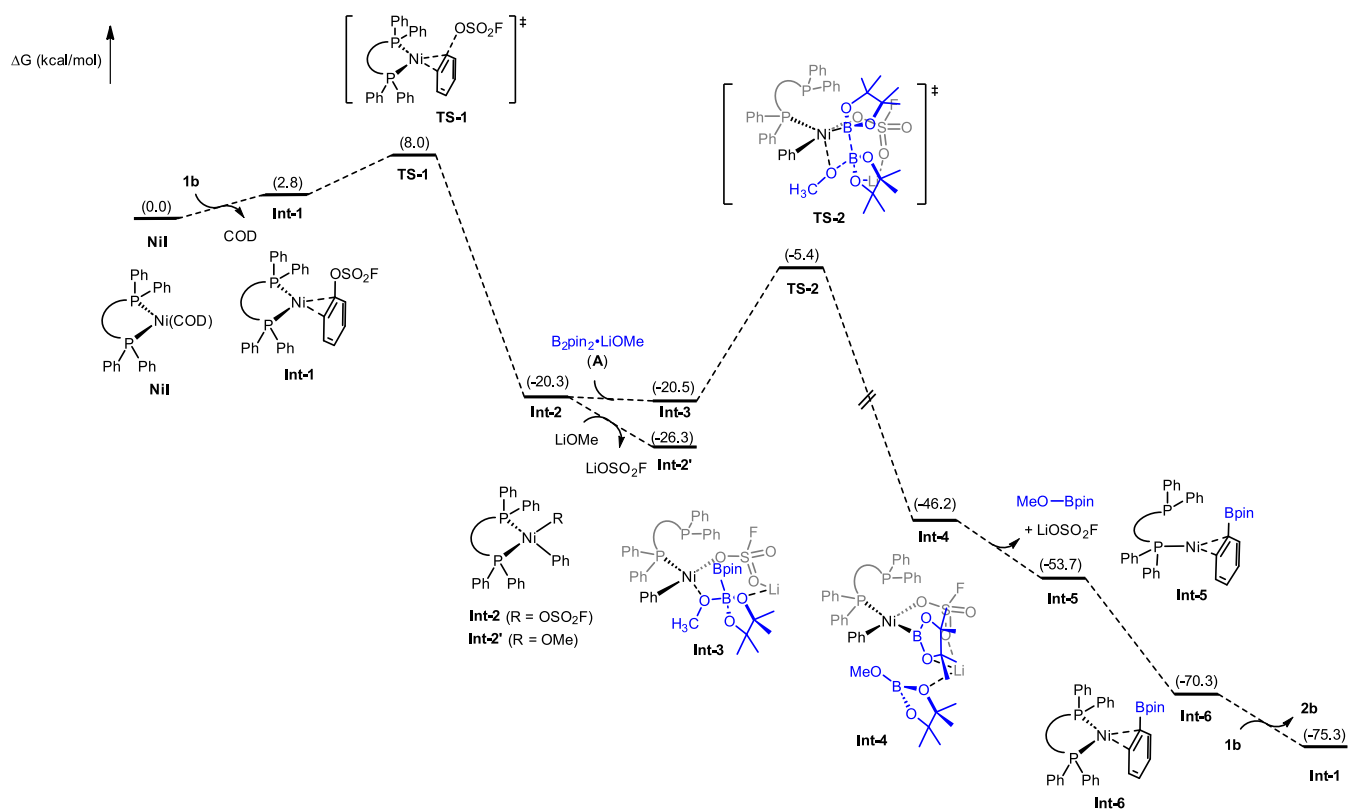


Figure 1. Calculated free-energy profile for the nickel-catalyzed borylation of aryl fluorosulfate **1b**. All calculations were performed at the SMD(DME)/M06/SDD(Ni, Fe)/6-311++G**//B3LYP-D3/LANL2DZ(Ni, Fe)/6-31G* level of theory. Energies are given in kcal/mol.

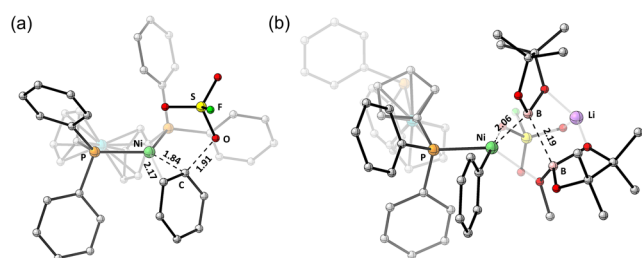


Figure 2. Optimized structures of selected TSs in Figure 1: (a) TS-1 and (b) TS-2.

oxidative addition complex Ni3', underwent disappearance within approximately 3 h to give Ni3 via the ligand exchange by pivalate.

In order to obtain the isolable LArNi(OSO₂F) complex, we postulated that the introduction of substituents on the aryl fluorosulfate **4** might confer enhanced stability, as exemplified by the work of the Diao group.^{42,43} To our delight, oxidative addition complexes Ni4a and Ni4b were successfully prepared by reacting aryl fluorosulfates **4a** and **4b** with Ni2 (Figure 4a). It is noteworthy that oxidative addition across the C–O bond of aryl fluorosulfates **4a** and **4b** proceeded smoothly, reaching full conversion within 1 h of reaction time, affording the corresponding complexes Ni4a or Ni4b in 92 and 95% isolated yield, respectively. These complexes were fully characterized by spectroscopic analysis, revealing distinct features in the ³¹P NMR spectra. Specifically, well-defined doublet signals were observed, indicative of a square planar d⁸ nickel complex.^{40,44} Moreover, a single-crystal X-ray structure was successfully determined for the complex Ni4b', where the anionic OSO₂F group was displaced by an acetonitrile molecule during the

crystal growth process.⁴⁵ These experimental results provide direct evidence of oxidative addition across the C–OSO₂F bond of aryl fluorosulfate **4b** by LNi(0), which aligns with the computational data mentioned earlier.

Then, our attention was shifted to the reactivity of the oxidative addition complexes. However, stoichiometric borylation with complex Ni4 yielded only a trace amount of desired product **5** (Figure 4b). Instead of stoichiometric reactivity of Ni4, we evaluated the performance of Ni4 in catalytic borylation of **1a** (Figure 4c), on the basis of Jamison and Doyle's previous studies that utilize the oxidative addition Ni(II) complexes as precatalysts.^{46,47} Notably, these reactions gave borylated product **2a** in moderate yields under standard conditions.

In our subsequent experiments utilizing Ni2 and aryl fluorosulfate **1a**, our aim was to investigate the role of the lithium ion in this borylation reaction. Control experiments were performed by adjusting the equivalents of 12-crown-4, a known lithium-ion capture agent. As depicted in Scheme 2, the graph shows that as the quantity of 12-crown-4 relative to LiOMe increases, the yield of **2a** decreases. This observation implies that the lithium ions are crucial for stabilizing the TS-2 in accordance with findings from DFT studies.^{42,43} Additionally, we observed that substituting LiOMe with NaOMe or KOMe (see also the Supporting Information, Table S3) led to the diminished reaction yields.

Based on the combined DFT experimental studies and the literature reports,^{48–52} we propose a plausible reaction mechanism for this Ni-catalyzed borylation of aryl fluorosulfates. The initial step of the catalytic cycle involves the oxidative addition step of LNi(0) across the C–O bond of aryl fluorosulfate to give LArNi(OSO₂F). This enables an alternative reactivity of SuFExable substrates, which were previously

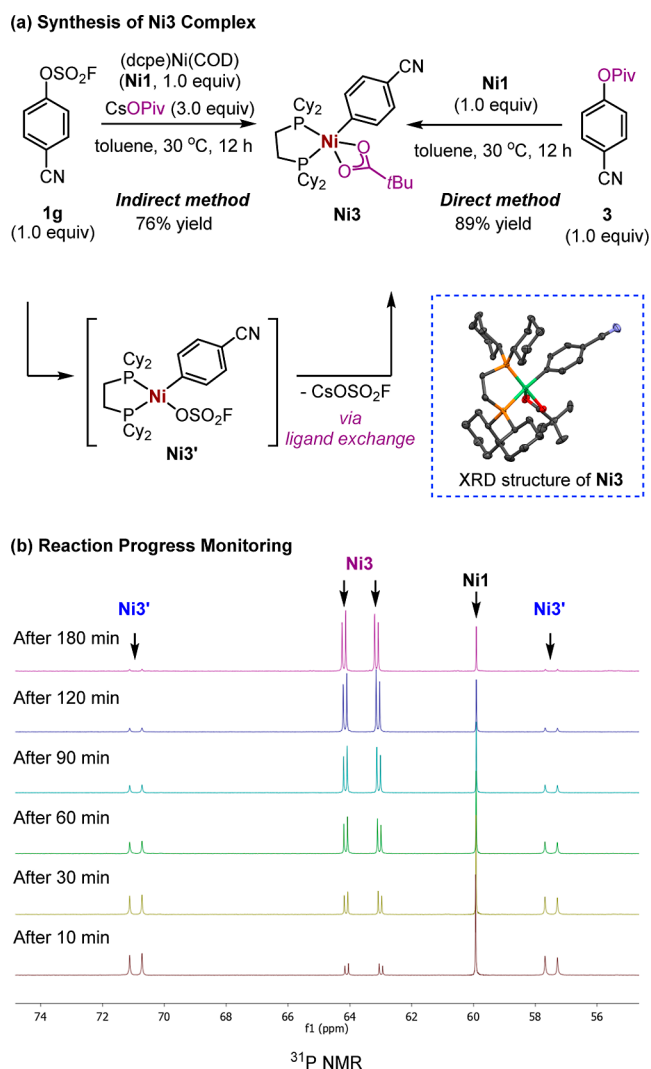


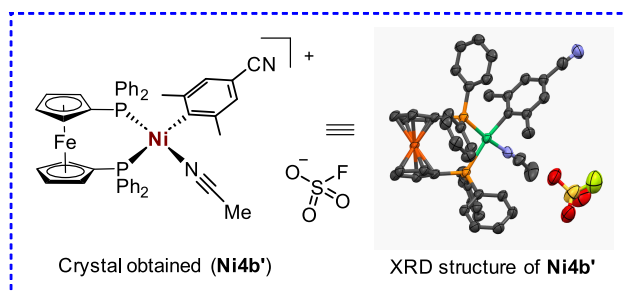
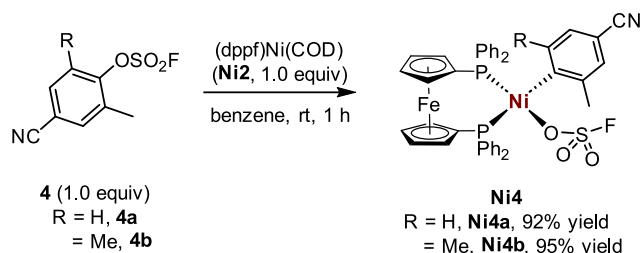
Figure 3. Synthesis of (dcpe)ArNiX complexes. (a) Synthesis of Ni3 by direct and indirect methods. (b) Monitoring the reaction progress between Ni1 and 1g in the presence of CsOPiv by ^{31}P NMR (162 MHz, toluene- d_8).

primarily focused on S–F bond functionalization. Following the oxidative addition step, the transmetalation step occurs where an activated $\text{B}_2\text{pin}_2\cdot\text{LiOMe}$ adduct transfers a boryl group to the $\text{LArNi}(\text{OSO}_2\text{F})$ complex, generating a $\text{LArNi}(\text{Bpin})$ complex. Finally, the reductive elimination of the complex yields the aryl boronate ester, while regenerating the Ni(0) active catalyst.

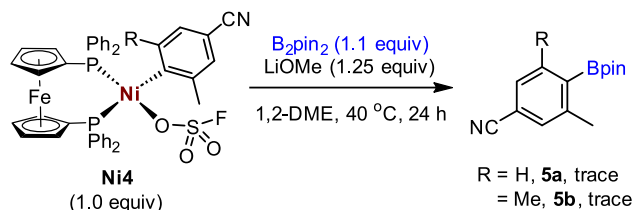
3. SUMMARY AND CONCLUSIONS

In this work, we successfully demonstrated a catalytic approach for transforming aryl fluorosulfates into aryl boronate esters. The reaction conditions are mild and require a low catalyst loading. Well-defined arylnickel(II) species, obtained from the oxidative addition of aryl fluorosulfates, were isolated for the first time, and their catalytic activities were examined. DFT calculations indicate that the direct transfer of the Bpin moiety from the activated boronate ester to the arylnickel(II) intermediate is operative via the unique lithium-bridged transition state. We anticipate that the combined experimental and computational studies will enhance our understanding of catalytic intermediates. These findings can serve as the foundation for rational

(a) Synthesis of Ni4 Complexes



(b) Stoichiometric Borylation Study Using Ni4



(c) Catalytic Borylation Study Using Ni4

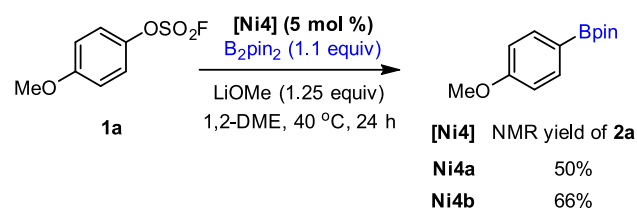


Figure 4. Synthesis of (dppf)ArNiX complexes and reactivity studies. (a) Synthesis of (dppf)ArNi(OSO₂F) Ni4 by reacting Ni2 and 4. (b) Stoichiometric borylation reaction of Ni4. (c) Catalytic reactivity of Ni4 in the borylation reaction. NMR yields were obtained by using mesitylene as an internal standard.

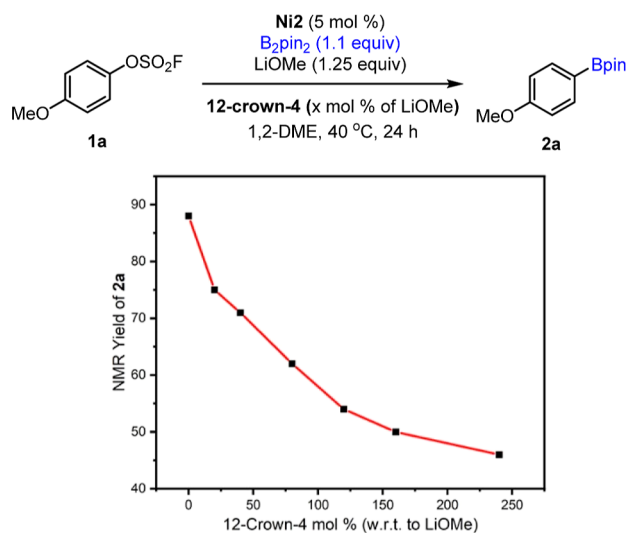
catalytic system design associated with organic synthesis, particularly for less explored substrates.

4. METHODS

4.1. General Borylation Procedure

In a N_2 -filled glovebox, a 4 mL vial equipped with a magnetic stir bar was charged with (dppf)Ni(COD) (Ni2) (5 mol %), bis(pinacolato)diboron (1.1 equiv), and LiOMe (1.25 equiv), followed by 1,2-DME. The mixture was then stirred at 40 °C for 15 min on a preheated metallic block. Subsequently, aryl fluorosulfate (1.0 equiv) was added. After stirring for 24 h at 40 °C, the reaction mixture was transferred to a 50 mL round-bottomed flask containing 20 mL of diethyl ether. After stirring for an additional 15 min at rt, the mixture was filtered through a short pad of Celite and washed thoroughly with diethyl ether (10 mL \times 2). The combined filtrate was concentrated in vacuo. The corresponding aryl boronic ester was isolated by flash column

Scheme 2. Role of Lithium Ions in the Catalytic Activity



chromatography using boric acid-impregnated silica gel to obtain the desired product.

■ ASSOCIATED CONTENT

Supporting Information

The Supporting Information is available free of charge at <https://pubs.acs.org/doi/10.1021/jacsau.4c00128>.

Experimental procedures, experimental and computational details, characterization data, spectra for all new compounds, crystallographic data, and Cartesian coordinates of all-computed structures (PDF)
 Crystallographic data for Ni3 (CIF)
 Crystallographic data for Ni4b' (CIF)

■ AUTHOR INFORMATION

Corresponding Authors

Byunghyuck Jung – Department of Physics and Chemistry, Daegu Gyeongbuk Institute of Science and Technology (DGIST), Daegu 42988, Republic of Korea; orcid.org/0000-0002-8582-082X; Email: byunghyuck.jung@dgist.ac.kr

Jaesung Kwak – Infectious Diseases Therapeutic Research Center, Korea Research Institute of Chemical Technology (KRICT), Division of Medicinal Chemistry and Pharmacology, KRICT School, University of Science and Technology (UST), Daejeon 34114, Republic of Korea; orcid.org/0000-0001-8010-7307; Email: jkwak@kRICT.re.kr

Sung You Hong – Department of Chemistry, Ulsan National Institute of Science and Technology (UNIST), Ulsan 44919, Republic of Korea; orcid.org/0000-0002-5785-4475; Email: syhong@unist.ac.kr

Authors

Manoj Kumar Sahoo – Department of Chemistry, Ulsan National Institute of Science and Technology (UNIST), Ulsan 44919, Republic of Korea

Jeong Woo Lee – Department of Chemistry, Ulsan National Institute of Science and Technology (UNIST), Ulsan 44919, Republic of Korea

Soochan Lee – Department of Chemistry, Ulsan National Institute of Science and Technology (UNIST), Ulsan 44919, Republic of Korea

Wonyoung Choe – Department of Chemistry, Ulsan National Institute of Science and Technology (UNIST), Ulsan 44919, Republic of Korea; orcid.org/0000-0003-0957-1187

Complete contact information is available at:

<https://pubs.acs.org/10.1021/jacsau.4c00128>

Author Contributions

M.K.S., B.J., J.K., and S.Y.H. conceived the project. M.K.S. and J.W.L. conducted the experiments. S.L. and W.C. obtained and analyzed the single-crystal XRD structure data. J.K. carried out the DFT calculations. All authors analyzed and interpreted the results. The manuscript was written through the contributions of all authors. All authors have given their approval to the final version of the manuscript. CRediT: **Manoj Kumar Sahoo** conceptualization, formal analysis, investigation, methodology, writing-original draft, writing-review & editing; **Jeong Woo Lee** data curation, formal analysis, writing-review & editing; **Soochan Lee** formal analysis, investigation, writing-original draft, writing-review & editing; **Wonyoung Choe** data curation, formal analysis, investigation, writing-original draft, writing-review & editing; **Byunghyuck Jung** conceptualization, data curation, formal analysis, investigation, writing-original draft, writing-review & editing; **Jaesung Kwak** conceptualization, data curation, formal analysis, funding acquisition, software, validation, writing-original draft, writing-review & editing; **Sung You Hong** conceptualization, formal analysis, funding acquisition, investigation, methodology, project administration, supervision, writing-original draft, writing-review & editing.

Notes

The authors declare no competing financial interest.

■ ACKNOWLEDGMENTS

We thank Professor Joong-Hyun Chun for discussions and valuable suggestions. This research was supported by the National Research Foundation of Korea (NRF) grant funded by the Korea government (MSIT) (NRF-2023R1A2C1004563, NRF-2020M3H4A3081883, and NRF-2020R1A5A1019631) and R&D research program of the Institutional Research Program of KRICT (KK2432-10). Single-crystal XRD experiments with synchrotron radiation were performed at the BL2D-SMC in the Pohang Accelerator Laboratory.

■ REFERENCES

- Hall, D. G. *Boronic Acids: Preparation and Applications in Organic Synthesis Medicine and Materials*, 2nd ed.; Wiley VCH: Weinheim, Germany, 2011; pp 1–133.
- Rygas, J. P. G.; Crudden, C. M. Enantiospecific and Iterative Suzuki-Miyaura Cross-Couplings. *J. Am. Chem. Soc.* **2017**, *139*, 18124–18137.
- Fyfe, J. W. B.; Watson, A. J. B. Recent Developments in Organoboron Chemistry: Old Dogs, New Tricks. *Chem* **2017**, *3*, 31–55.
- Neeve, E. C.; Geier, S. J.; Mkhaliid, I. A. I.; Westcott, S. A.; Marder, T. B. Diboron(4) Compounds: From Structural Curiosity to Synthetic Workhorse. *Chem. Rev.* **2016**, *116*, 9091–9161.
- Bhanuchandra, M.; Baralle, A.; Otsuka, S.; Nogi, K.; Yorimitsu, H.; Osuka, A. Palladium-Catalyzed ipso-Borylation of Aryl Sulfides with Diborons. *Org. Lett.* **2016**, *18*, 2966–2969.
- Semba, K.; Fujihara, T.; Terao, J.; Tsuji, Y. Copper-Catalyzed Borylative Transformations of Non-Polar Carbon-Carbon Unsaturated

Compounds Employing Borylcopper as an Active Catalyst Species. *Tetrahedron* **2015**, *71*, 2183–2197.

(7) Choy, P. Y.; Tse, M. H.; Kwong, F. Y. Recent Expedition in Pd- and Rh-Catalyzed C_(Ar)-B Bond Formations and Their Applications in Modern Organic Syntheses. *Chem.—Asian J.* **2023**, *18*, No. e202300649.

(8) Bose, S. K.; Mao, L.; Kuehn, L.; Radius, U.; Nekvinda, J.; Santos, W. L.; Westcott, S. A.; Steel, P. G.; Marder, T. B. First-Row d-Block Element-Catalyzed Carbon-Boron Bond Formation and Related Processes. *Chem. Rev.* **2021**, *121*, 13238–13341.

(9) Wang, M.; Shi, Z. Methodologies and Strategies for Selective Borylation of C-Het and C-C Bonds. *Chem. Rev.* **2020**, *120*, 7348–7398.

(10) Chow, W. K.; Yuen, O. Y.; Choy, P. Y.; So, C. M.; Lau, C. P.; Wong, W. T.; Kwong, F. Y. A Decade Advancement of Transition Metal-Catalyzed Borylation of Aryl Halides and Sulfonates. *RSC Adv.* **2013**, *3*, 12518–12539.

(11) Malapit, C. A.; Bour, J. R.; Laursen, S. R.; Sanford, M. S. Mechanism and Scope of Nickel-Catalyzed Decarbonylative Borylation of Carboxylic Acid Fluorides. *J. Am. Chem. Soc.* **2019**, *141*, 17322–17330.

(12) Molander, G. A.; Cavalcanti, L. N.; García-García, C. Nickel-Catalyzed Borylation of Halides and Pseudohalides with Tetrahydroxydiboron [B₂(OH)₄]. *J. Org. Chem.* **2013**, *78*, 6427–6439.

(13) Boit, T. B.; Bulger, A. S.; Dander, J. E.; Garg, N. K. Activation of C-O and C-N Bonds Using Non-Precious-Metal Catalysis. *ACS Catal.* **2020**, *10*, 12109–12126.

(14) Tobisu, M.; Chatani, N. Cross-Couplings Using Aryl Ethers via C-O Bond Activation Enabled by Nickel Catalysts. *Acc. Chem. Res.* **2015**, *48*, 1717–1726.

(15) Bae, J.; Cho, E. J. P,N Ligand in Ni-Catalyzed Cross-Coupling Reactions: A Promising Tool for π -Functionalization. *ACS Catal.* **2023**, *13*, 13540–13560.

(16) Hsu, C.-M.; Lin, H.-B.; Hou, X.-Z.; Tapales, R. V. P. P.; Shih, C.-K.; Minoza, S.; Tsai, Y.-S.; Tsai, Z.-N.; Chan, C.-L.; Liao, H.-H. Azetidines with All-Carbon Quaternary Centers: Merging Relay Catalysis with Strain Release Functionalization. *J. Am. Chem. Soc.* **2023**, *145*, 19049–19059.

(17) Zhu, C.; Kale, A. P.; Yue, H.; Rueping, M. Redox-Neutral Cross-Coupling Amination with Weak N-Nucleophiles: Arylation of Anilines, Sulfonamides, Sulfoximines, Carbamates, and Imines via Nickel-alectrocatalysis. *JACS Au* **2021**, *1*, 1057–1065.

(18) Diccianni, J. B.; Diao, T. Mechanisms of Nickel-Catalyzed Cross-Coupling Reactions. *Trends Chem.* **2019**, *1*, 830–844.

(19) Mohadjer Beromi, M.; Nova, A.; Balcells, D.; Brasacchio, A. M.; Brudvig, G. W.; Guard, L. M.; Hazari, N.; Vinyard, D. J. Mechanistic Study of an Improved Ni Precatalyst for Suzuki-Miyaura Reactions of Aryl Sulfamates: Understanding the Role of Ni(I) Species. *J. Am. Chem. Soc.* **2017**, *139*, 922–936.

(20) Liu, X.; Xu, B.; Su, W. Ni-Catalyzed Deoxygenative Borylation of Phenols Via O-Phenyl-uronium Activation. *ACS Catal.* **2022**, *12*, 8904–8910.

(21) Qiu, Z.; Li, C.-J. Transformations of Less-Activated Phenols and Phenol Derivatives via C-O Cleavage. *Chem. Rev.* **2020**, *120*, 10454–10515.

(22) Zeng, H.; Qiu, Z.; Domínguez-Huerta, A.; Hearne, Z.; Chen, Z.; Li, C.-J. An Adventure in Sustainable Cross-Coupling of Phenols and Derivatives via Carbon-Oxygen Bond Cleavage. *ACS Catal.* **2017**, *7*, 510–519.

(23) Rosen, B. M.; Quasdorf, K. W.; Wilson, D. A.; Zhang, N.; Resmerita, A.-M.; Garg, N. K.; Percec, V. Nickel-Catalyzed Cross-Couplings Involving Carbon-Oxygen Bonds. *Chem. Rev.* **2011**, *111*, 1346–1416.

(24) Wilson, D. A.; Wilson, C. J.; Moldoveanu, C.; Resmerita, A. M.; Corcoran, P.; Hoang, L. M.; Rosen, B. M.; Percec, V. Neopentylglycolborylation of Aryl Mesylates and Tosylates Catalyzed by Ni-Based Mixed-Ligand Systems Activated with Zn. *J. Am. Chem. Soc.* **2010**, *132*, 1800–1801.

(25) Huang, K.; Yu, D.-G.; Zheng, S.-F.; Wu, Z.-H.; Shi, Z.-J. Borylation of Aryl and Alkenyl Carbamates through Ni-Catalyzed C-O Activation. *Chem.—Eur. J.* **2011**, *17*, 786–791.

(26) Zarate, C.; Manzano, R.; Martin, R. Ipso-Borylation of Aryl Ethers via Ni-Catalyzed C-OMe Cleavage. *J. Am. Chem. Soc.* **2015**, *137*, 6754–6757.

(27) Zeng, X.; Zhang, Y.; Liu, Z.; Geng, S.; He, Y.; Feng, Z. Iron-Catalyzed Borylation of Aryl Ethers via Cleavage of C-O Bonds. *Org. Lett.* **2020**, *22*, 2950–2955.

(28) Pein, W. L.; Wiensch, E. M.; Montgomery, J. Nickel-Catalyzed Ipso-Borylation of Silyloxyarenes via C-O Bond Activation. *Org. Lett.* **2021**, *23*, 4588–4592.

(29) Liu, X.; Xu, B.; Su, W. Ni-Catalyzed Deoxygenative Borylation of Phenols Via O-Phenyluronium Activation. *ACS Catal.* **2022**, *12*, 8904–8910.

(30) Dong, J.; Krasnova, L.; Finn, M. G.; Sharpless, K. B. Sulfur(VI) Fluoride Exchange (SuFEx): Another Good Reaction for Click Chemistry. *Angew. Chem., Int. Ed.* **2014**, *53*, 9430–9448.

(31) Dong, J.; Sharpless, K. B.; Kwisnek, L.; Oakdale, J. S.; Fokin, V. V. SuFEx-Based Synthesis of Polysulfates. *Angew. Chem., Int. Ed.* **2014**, *53*, 9466–9470.

(32) Gao, B.; Zhang, L.; Zheng, Q.; Zhou, F.; Klivansky, L. M.; Lu, J.; Liu, Y.; Dong, J.; Wu, P.; Sharpless, K. B. Bifluoride-Catalyzed Sulfur(VI) Fluoride Exchange Reaction for the Synthesis of Polysulfates and Polysulfonates. *Nat. Chem.* **2017**, *9*, 1083–1088.

(33) Lou, T. S.-B.; Willis, M. C. Sulfonyl Fluorides as Targets and Substrates in the Development of New Synthetic Methods. *Nat. Rev. Chem.* **2022**, *6*, 146–162.

(34) Liang, Q.; Xing, P.; Huang, Z.; Dong, J.; Sharpless, K. B.; Li, X.; Jiang, B. Palladium-Catalyzed, Ligand-Free Suzuki Reaction in Water Using Aryl Fluorosulfates. *Org. Lett.* **2015**, *17*, 1942–1945.

(35) Hanley, P. S.; Clark, T. P.; Krasovskiy, A. L.; Ober, M. S.; O'Brien, J. P.; Staton, T. S. Palladium- and Nickel-Catalyzed Amination of Aryl Fluorosulfonates. *ACS Catal.* **2016**, *6*, 3515–3519.

(36) Ma, C.; Zhao, C. Q.; Xu, X. T.; Li, Z. M.; Wang, X. Y.; Zhang, K.; Mei, T. S. Nickel-Catalyzed Carboxylation of Aryl and Heteroaryl Fluorosulfates Using Carbon Dioxide. *Org. Lett.* **2019**, *21*, 2464–2467.

(37) Lekkala, R.; Lekkala, R.; Moku, B.; Rakesh, K. P.; Qin, H. L. Applications of Sulfuryl Fluoride (SO₂F₂) in Chemical Transformations. *Org. Chem. Front.* **2019**, *6*, 3490–3516.

(38) Saraswat, S. K.; Seemaladinne, R.; Abdullah, M. N.; Zaini, H.; Ahmad, N.; Ahmad, N.; Vessally, E. Aryl Fluorosulfates: Powerful and Versatile Partners in Cross-Coupling Reactions. *RSC Adv.* **2023**, *13*, 13642–13654.

(39) Na, J.-H.; Liu, X.; Jing, J.-W.; Wang, J.; Chu, X.-Q.; Ma, M.; Xu, H.; Zhou, X.; Shen, Z.-L. Nickel-Catalyzed Direct Cross-Coupling of Aryl Fluorosulfates with Aryl Bromides. *Org. Lett.* **2023**, *25*, 2318–2322.

(40) Muto, K.; Yamaguchi, J.; Lei, A.; Itami, K. Isolation, Structure, and Reactivity of an Arylnickel(II) Pivalate Complex in Catalytic C-H/C-O Biaryl Coupling. *J. Am. Chem. Soc.* **2013**, *135*, 16384–16387.

(41) The complex was prepared according to the literature procedure reported by Itami group, ref 40.

(42) Lin, Q.; Diao, T. Mechanism of Ni-Catalyzed Reductive 1,2-Dicarbonylfunctionalization of Alkenes. *J. Am. Chem. Soc.* **2019**, *141*, 17937–17948.

(43) Lin, Q.; Spielvogel, E. H.; Diao, T. Carbon-Centered Radical Capture at Nickel(II) Complexes: Spectroscopic Evidence, Rates, and Selectivity. *Chem* **2023**, *9*, 1295–1308.

(44) Boehm, P.; Müller, P.; Finkelstein, P.; Rivero-Crespo, M. A.; Ebert, M.-O.; Trapp, N.; Morandi, B. Mechanistic Investigation of the Nickel-Catalyzed Metathesis between Aryl Thioethers and Aryl Nitriles. *J. Am. Chem. Soc.* **2022**, *144*, 13096–13108.

(45) A mixture of acetonitrile and hexane in 1:50 ratio was used to yield the crystal suitable for single crystal XRD; for details procedure, see the [Supporting Information](#).

(46) Standley, E. A.; Jamison, T. F. Simplifying Nickel(0) Catalysis: An Air-Stable Nickel Precatalyst for the Internally Selective Benzylolation of Terminal Alkenes. *J. Am. Chem. Soc.* **2013**, *135*, 1585–1592.

(47) Shields, J. D.; Gray, E. E.; Doyle, A. G. A Modular, Air-Stable Nickel Precatalyst. *Org. Lett.* **2015**, *17*, 2166–2169.

(48) Russell, J. E. A.; Entz, E. D.; Joyce, I. M.; Neufeldt, S. R. Nickel-Catalyzed Stille Cross Coupling of C-O Electrophiles. *ACS Catal.* **2019**, *9*, 3304–3310.

(49) Roh, B.; Farah, A. O.; Kim, B.; Feoktistova, T.; Moeller, F.; Kim, K. D.; Cheong, P. H.-Y.; Lee, H. G. Stereospecific Acylative Suzuki-Miyaura Cross-Coupling: General Access to Optically Active α -Aryl Carbonyl Compounds. *J. Am. Chem. Soc.* **2023**, *145*, 7075–7083.

(50) Yin, G.; Kalvet, I.; Englert, U.; Schoenebeck, F. Fundamental Studies and Development of Nickel Catalyzed Trifluoromethylthiolation of Aryl Chlorides: Active Catalytic Species and Key Roles of Ligand and Traceless MeCN Additive Revealed. *J. Am. Chem. Soc.* **2015**, *137*, 4164–4172.

(51) Guard, L. M.; Mohadjer Beromi, M.; Brudvig, G. W.; Hazari, N.; Vinyard, D. J. Comparison of dppf-Supported Nickel Precatalysts for the Suzuki-Miyaura Reaction: The Observation and Activity of Nickel(I). *Angew. Chem., Int. Ed.* **2015**, *54*, 13352–13356.

(52) Bajo, S.; Laidlaw, G.; Kennedy, A. R.; Sproules, S.; Nelson, D. J. Oxidative Addition of Aryl Electrophiles to a Prototypical Nickel(0) Complex: Mechanism and Structure/Reactivity Relationships. *Organometallics* **2017**, *36*, 1662–1672.